Dynamics of Atmospheres and Oceans 46 (2009) 36–45

Contents lists available at ScienceDirect

Dynamics of Atmospheres and Oceans

journal homepage: www.elsevier.com/locate/dynatmoce

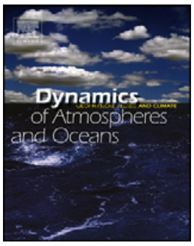

Filament generation off the Strait of Gibraltar in response to Gap winds

Álvaro Peliz[a,*], Ana Teles-Machado[b], Patrick Marchesiello[c], Jesus Dubert[b], Jesus Garcia Lafuente[d]

[a] Instituto de Oceanografia, Universidade de Lisboa, Lisboa, Portugal
[b] Departamento de Fisica (CESAM), Universidade de Aveiro, 3810-193 Aveiro, Portugal
[c] Institut de Recherche pour le Développement, Noumea, New Caledonia
[d] Departamento de Fisica Aplicada II, Universidad de Malaga, Campus de Teatinos, 29071 Malaga, Spain

ARTICLE INFO

Article history:
Received 9 April 2008
Received in revised form 16 July 2008
Accepted 13 August 2008
Available online 26 August 2008

Keywords:
Strait of Gibraltar
Filaments
Gap winds

ABSTRACT

We present a case study of the generation of a cold filament rooted off the southwestern edge of the Strait of Gibraltar (Atlantic side) during the summer of 2000. The event is successfully simulated using high-resolution atmospheric and oceanic numerical models. It is shown that a sharp filament may develop oceanwards with little modification of the Atlantic inflow into the Mediterranean, contrary to usual expectations. The filament is essentially driven by the surface layer response to Gap winds occurring during Levanter conditions. The easterly wind funnelling in the Strait generates a strong wind jet and intense wind curl which impacts the oceanic surface layer through Ekman pumping and mixing processes. The generation and fate of the filament is very similar to the Gulf of Tehuantepec case, where strong Gap wind events produce asymmetric deformation and erosion of the thermocline that tends to favour anticyclonic mesoscale circulations. Our observations and model results from both realistic and idealized experiments suggest that similar phenomena are present in the Gulf of Cadiz, but they are altered by the persisting Atlantic inflow, so that the response to Gap winds is not as dramatic.

* Corresponding author.
E-mail address: ajpeliz@fc.ul.pt (Á. Peliz).

0377-0265/$ – see front matter © 2008 Elsevier B.V. All rights reserved.
doi:10.1016/j.dynatmoce.2008.08.002

1. Introduction

The subinertial flow in the Strait of Gibraltar (Fig. 1) consists of several concurring processes including the direct action of winds along or in the vicinity of the Strait (Garcia Lafuente et al., 2002a; Menemenlis et al., 2007). A recurrent sea surface temperature (SST) pattern in satellite imagery of the Gibraltar zone is a cold water band along the south side of the Strait, that eventually develops westward (Atlantic side) generating a filament protruding into the Gulf of Cadiz (Folkard et al., 1997; Stanichny et al., 2005). This feature has been associated with the occurrence of easterly winds, that accelerating through the strait, oppose the dominant inflow, and, concomitantly with atmospheric pressure forcing, could stop and reverse it (Garcia Lafuente et al., 2002b). Stanichny et al. (2005) describe an event using SST images from the summer 2003, and conclude that the easterlies event may temporarily revert the inflow since the upwelled water is seemingly transported to the Atlantic Ocean, then back again into the Strait when the winds relax. According to Stanichny et al. (2005), the filament is generated during this process. In the present study, we show that the formation of the cold filament is not necessarily associated with inflow shutoff or reversal, and we propose a different process essentially associated with the stratified upper layer response to intense Gap winds. The proposed mechanism is very similar to what occurs in the Gulf of Tehuantepec (Eastern tropical Pacific), where Ekman pumping and mixing driven by strong wind jets can generate offhsore upwelling filaments and associated eddy features (see Willett et al. (2006) for a review). However, in our case, the generation of warm core anticyclonic eddies is altered by the persisting Atlantic inflow. Our study is based on an oceanic and atmospheric modeling simulation of August 2000 during an easterlies event in the Strait of Gibraltar.

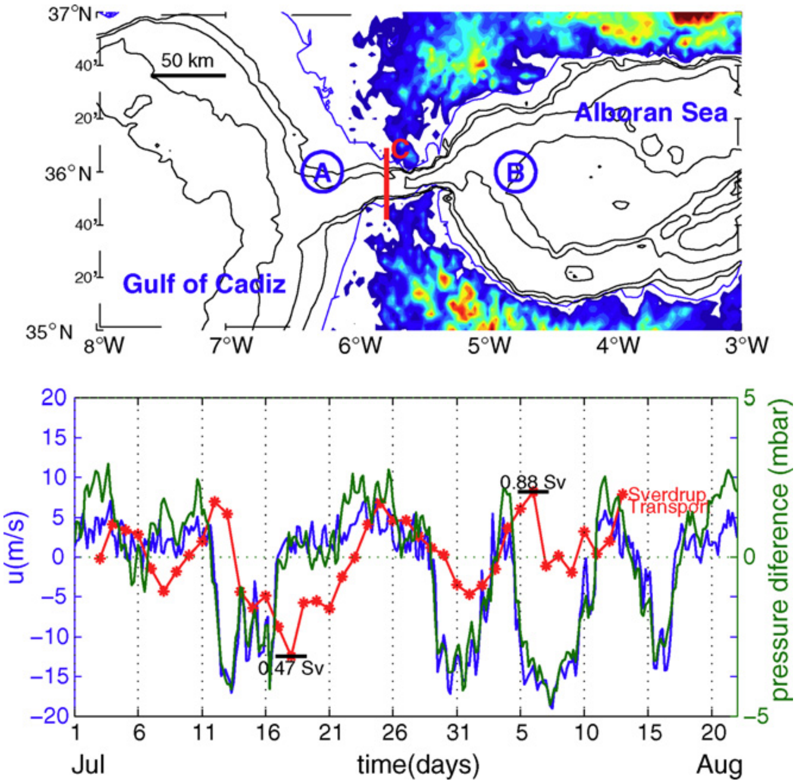

Fig. 1. Top: Map of the Strait of Gibraltar and model Domain. Orography over land is represented in color, and ocean topography is shown by the 200, 400 and 1000 m isobaths. The thick lines show the locations of the ocean model sections referred to in the text and other figures. Point A and B indicate the sites where the time series of the Meteorological model were extracted. Bottom: Time series of along Strait winds (zonal component, blue line) and atmospheric sea surface pressure difference along the Strait between points A and B (green line). Time series of model inflow transport in Sv calculated for Section C (red line). (For interpretation of the references to color in this figure legend, the reader is referred to the web version of the article.)

2. Atmosphere and Ocean simulations

The simulations were performed with the Regional Ocean Modeling System (ROMS; Shchepetkin and McWilliams, 2005) with nesting capabilities (Penven et al., 2006). ROMS is a 3D free-surface, sigma-coordinate, split-explicit primitive equation model with Boussinesq and hydrostatic approximations. A 3rd order accurate predictor-corrector – leapfrog/Adams-Moulton – time step algorithm is used which allows a substantial increase of time step as well as good dispersive properties for the advection equation. The open boundary conditions are a combination of outward radiation and flow-adaptive nudging toward prescribed external conditions either from climatology or from previous experiments (Marchesiello et al., 2001). Explicit lateral viscosity is null everywhere, except along sponge layers near open boundaries. Vertical mixing processes are parameterized with the non-local K-profile (KPP) boundary layer scheme (Large et al., 1994) implemented for both surface and bottom boundary layers. The vertical diffusion terms are treated with a semi-implicit, Crank-Nicholson scheme to avoid time step restrictions due to large vertical mixing rates in the boundary layers and also in the interior when static stability needs to be restored. A Smagorinsky scheme for lateral mixing and tracer diffusion is added allowing for a more realistic and selective temperature and salinity diffusion which produces a better model Mediterranean Outflow water masses. The numerical experiments are based on previous studies by Peliz et al. (2007, submitted for publication); Teles-Machado et al. (2007). The reader is referred to those studies for more detailed explanation of the model and configurations.

The simulations consist of two phases. In a first phase we aim at bringing the initial ocean conditions to a mean equilibrium solution representative of summer period (more specifically mean July conditions). The objective is to produce an initial state in which all the main circulation features are represented with the observed time and space scales of variability. To achieve this we conduct a series of climatological experiments using climatological temperature and salinity data, and forced by a climatologycal atmosphere (Marchesiello et al., 2003; Peliz et al., 2007, e.g.). In the specific case of the Strait of Gibraltar the high resolution required for explicit representation of the exchanged processes is incompatible (due to the available computational facilities) with the long spin-up time and large model domain required for an efficient spin-up. Since climatological inflow/outflow values are approximately known we conduct the spin-up phase in separate for the two basins (Atlantic and Mediterranean). The exactly same boundary condition is applied to both sides (in both configurations) to represent the inflow/outflow mean exchange. For the Atlantic side we use the initial fields of Peliz et al. (2007) which are extensively analyzed in Peliz et al. (submitted for publication). These initial fields were obtained using a set of grids on online and offline nesting (see Fig. 2 spin-up 1 and spin-up 2). The several scales involved in the representation of a realistic Mediterranean Outflow and circulation patterns in the Gulf of Cadiz required such a complex configuration setting. These initial states and circulations are thoroughly described in those papers and will not be repeated here. In what concerns the Mediterranean spin-up experiment, we have tested two different options: a larger/lower resolution (8 km) grid limited on the west by the longitudes of Sardinia Island, and a a smaller/higher resolution (4.5 km) domain (Spin-up 3 grid in Fig. 2). The results, though not significantely different, show a more realistic Aboran Sea Gyre in the smaller domain which was adopted for the initial and boundary conditions. The methodology used for the Mediterranean side spin-up, is the same as for the Atlantic. In both cases, the Gibraltar Strait is represented as a boundary condition with exactly the same prescribed values (see Peliz et al., 2007).

The obtained spin-up solutions provide monthly mean fields (because they are forced with monthly mean climatological atmosphere) which we adopt as initial (a climatological 1st July) and lateral boundaries for the period July–August. This lateral forcing is composed of temperature, salinity and momentum boundary data from the climatological runs, together with radiative conditions and passive–active relaxation (Marchesiello et al., 2001). This guarantees that over a mean beckground equilibrium solution, event scale fluctuations are allowed. Moreover, since the solution was forced by the same Gibraltar exchange condition, the inflow/outflow is also a part of that mean flow. The obtained initial and boundary data is then interpolated into a higher resolution grid encompassing both the Alboran and Gulf of Cadiz (Fig. 2 red box; $\sim$2 km resolution). This latter configuration set-up is the one that we use for the realistic simulation.

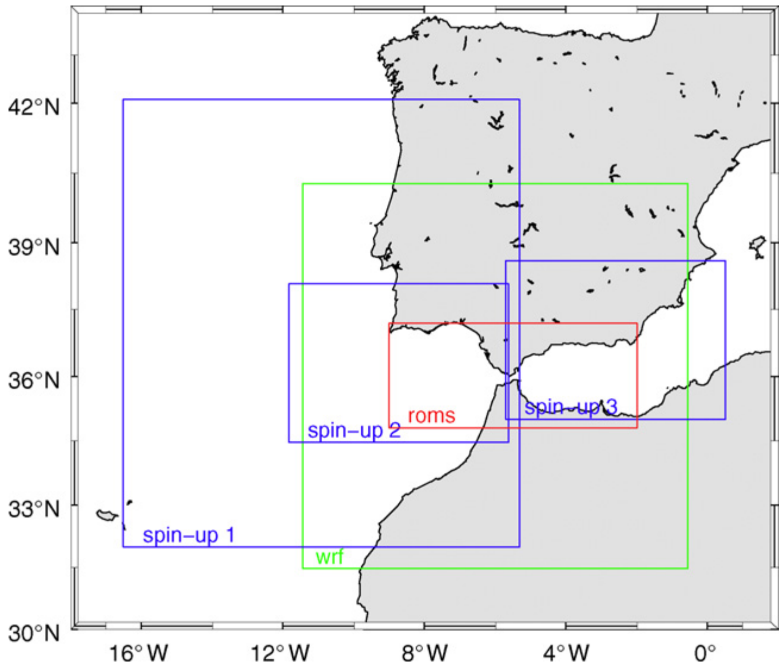

Fig. 2. Model grids used in the present configuration. The blue boxes indicate the domains used to calculate initial and boundary conditions during the spin-up experiments: spin-up 1 and spin-up 2 are the same as in Peliz et al. (2007), and have 7.5 and 2.6 km resolution, respectively. The Mediterranean side initial and boundary conditions were obtained with the spin-up 3 grid (4.5 km resolution). The resulting equilibrium solutions for summer (July–August) were interpolated into the 2 km resolution red grid used for the Gap wind event study. All ocean model grids have 60 sigma levels in the vertical. The green box indicates the 10 km resolution WRF simulation domain. (For interpretation of the references to color in this figure legend, the reader is referred to the web version of the article.)

The 2 month simulation covering the Gap wind event under study (July–August 2000) is forced with realistic atmospheric fields. The forcing conditions are produced with the Weather Research and Forecasting (WRF V2.0) model (Skamarock et al., 2005). The WRF simulations are initialized and forced along the boundaries with NCEP2 reanalysis. The atmospheric model is configured with a 10-km resolution grid (Fig. 2, green box). 46 vertical levels are used between the surface and 70 hPa pressure level. For physics parameterizations the options are standard (either default or recommended), including the Mellor–Yamada–Janjic TKE scheme for the planetary boundary layer. For the dynamics, the momentum equations are solved in non-hydrostatic mode, using third order Runge-Kutta time integration; fifth/third order spatial discretization for horizontal/vertical advection terms; and a Smagorinsky scheme for diffusion. The model is initialized by interpolating NCEP fields to the model grid. Along the integrations the boundaries are updated with six-hourly NCEP fields and the SST with weekly Reynolds SST values. See Teles-Machado et al. (2007) and Peliz et al. (submitted for publication) for two similar configurations details and comparison with observations.

In the present simulations we did not include tidal motions. Interactions exist between mesoscale and wind-driven processes on one hand and higher frequency tidal fluctuations (mostly semidiurnal) on the other hand. Vázquez et al. (2008) has recently shown that the periodic excitation of higher frequency internal waves by the bore generated between the mean inflow and outflow may break and increase the turbulent mixing between mean flows. Other small-scale mechanisms affecting vertical stratification in the Strait are mixing within the hydraulic transition downstream of the internal hydraulic jump formed in Camarinal sill (this is addressed by Send and Baschek (2001), among many others), and turbulent mixing induced by entrainment of the passive layer (Mediterranean in the eastern part, Atlantic in the western part) by the active, swift layer (Atlantic in the east, Mediterranean in the west). However, all these processes are not expected to significantly modify the bulk of the inflow response and we may consider them marginal for the case under study. This would be justified by the rapid damping of tidal fluctuations in the inflow at the eastern part of the Strait (Garcia Lafuente et al., 2000) and in the outflow at the westernmost section (Sánchez-Román et al., submitted for publication). It is a consequence of internal hydraulics of the strait, which maintain maximal exchange if the subcritical region of strong tidal activity (in the vicinity of the main sill of Camarinal) is bounded by critical sections at both ends of the Strait (Farmer and Armi, 1988). In this case, the subinertial variability of the flow is rather independent of the small scale processes taking place in the subcritical region (Armi and Farmer, 1987).

3. Results

3.1. The 2000 event from SST imagery and simulated winds

The evolution of SST fields (from satellite infrared observations) in the first week of August is represented in Fig. 3 (left column; days are 4th, 6th and 8th August). The images show the development of a sharp cold filament rooted at the southwest side of the Strait of Gibraltar. The filament starts to build up by 4th August and presents its full development by 8th August. The cold waters seem to originate inside the Strait by upwelling along its south coast—an evolution similar to the 2003 case reported in Stanichny et al. (2005). The filament extends westwards with a length in the order of 100 km and slightly curling anticyclonically. A small expansion to the south is also observed.

The surface wind fields (from WRF outputs) for the same days are represented in Fig. 3 and a time series of the along Strait winds is shown in Fig. 1. The series show three main events of strong easterlies with similar magnitude and duration. The events last about 5 days each and reach maximum values in the order of 15 m/s. It is worth noting that the correlation between the zonal component and the sea level presure (SLP) difference across the Strait is very high, especially during the easterlies events, showing the remarkable ageostrophic nature of winds in the vicinity of the Strait.

From the time series of Fig. 1, and from the surface winds in Fig. 3 (right column), we can see that an event starts developing by 5th August. The surface winds by 6th August show a jet that intensifies downstream of the Strait. The jet is almost zonally aligned and extends far westward to about 200 km. The core of the wind jet is slightly to the north of the Strait axis. Near the Strait, the jet exhibits a considerable meridional curl. By 8th August the jet axis looses its zonal alignment turning northward. In summary, the jet may be classified as a Gap wind event that occur in this region in association with Levanter conditions (easterlies): The air is forced by strong SLP gradients through the gap existing along

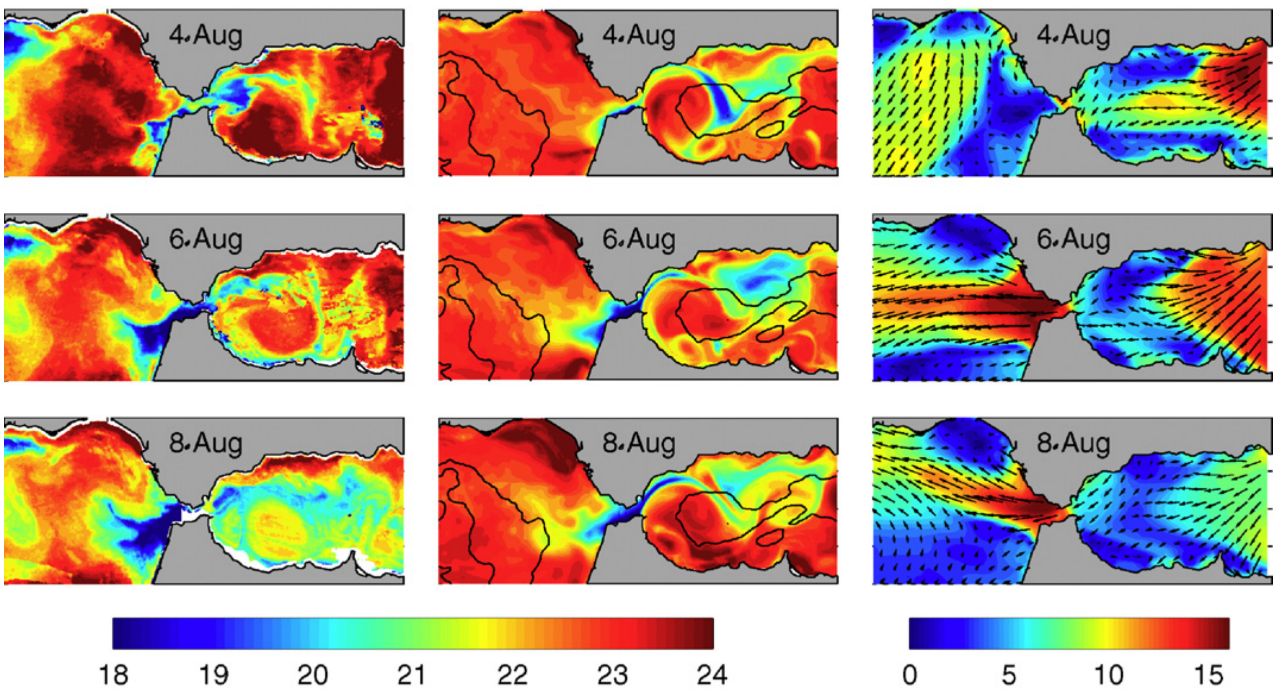

Fig. 3. Satellite and model (left and middle columns) Sea surface temperature (SST) fields showing the development of the filament from 4th to 8th August in the summer of 2000. Model (WRF) surface wind speed and vectors for the same dates (right column).

the Strait which is bordered by prominent topography (see Fig. 1). An example of synoptic situations prone to Gap wind development is presented by Palomares Losada (1999).

3.2. The model filaments and inflow variability

Model sea surface temperature fields for the same days as the satellite data are presented in Fig. 3 (middle column). The model simulates the main circulation patterns of both sides of the Strait as seen in satellite imagery. In the Mediterranean side, the Western Alboran Gyre, which results from Atlantic inflow interaction with topography, appears with its typically cold signature on the northern edge. In the Atlantic side, the cold filament which is the subject of the present study is also present. The Gibraltar Strait filament emerges in the model simulations at the same place and with similar scales as the observations. It is noticeable however, that the response in the model SST is weaker. By the time of full filament development (8th August) the oceanward extent and the anticyclonic curling of the model filament is very similar to the observations (Fig. 3).

To understand if the filament development is associated with any change in the inflow structure as suggested by Stanichny et al. (2005), the cross-strait flow dynamical structure is analyzed for the period before and at the peak of the event (Fig. 4). The adjusted inflow/outflow double circulation system that is typical of the Gibraltar Strait is clear in both situations. In the unperturbed case with no easterlies (by 27th July, Fig. 4a and c), the isopycnal slopes change at about 50 m depth, just on top of the main inflow core. Below 50 m depth, the isopycnals curve down towards the southern border. Above this depth, they are flat or have a slight outcrop. During the event of Gap winds (Fig. 4d and b), the isopycnals near the southern border bend upward, but no significant change in the bulk of the Atlantic inflow structure is observed. The response to the Gap wind is concentrated in the top

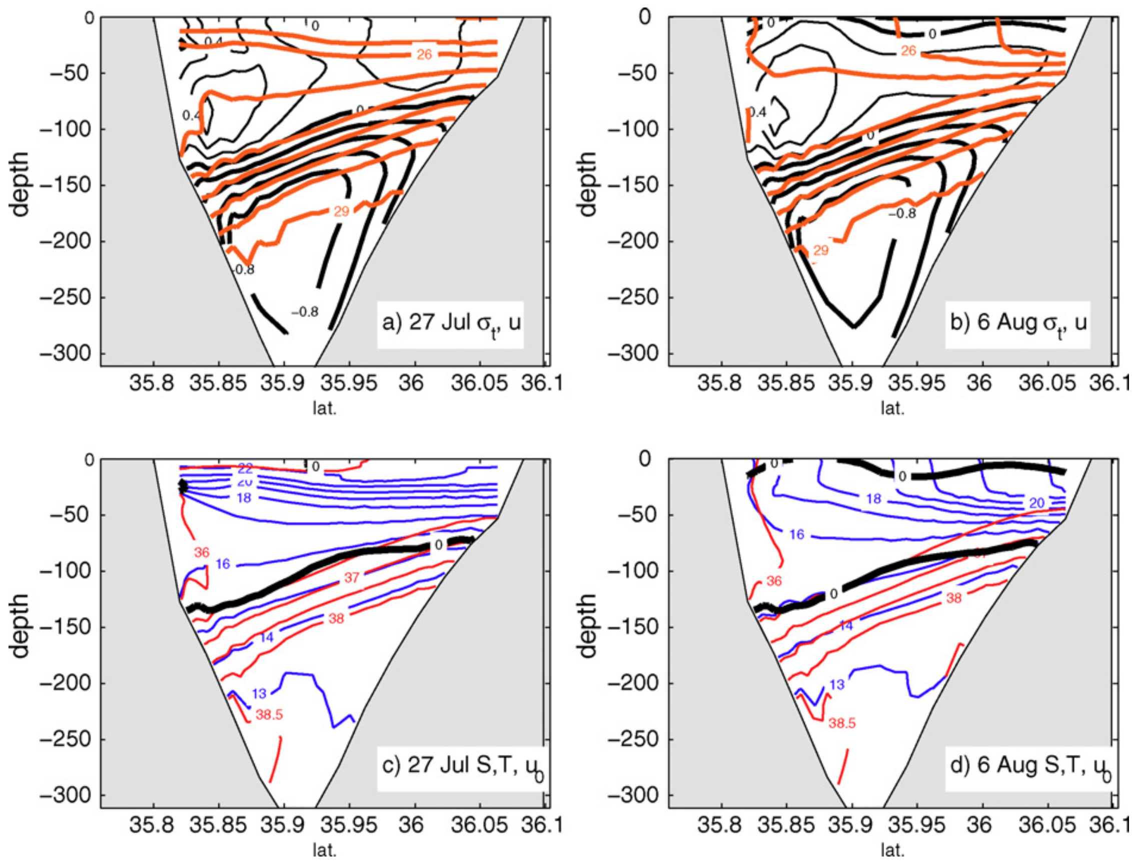

Fig. 4. Cross-strait sections (see Fig. 1 for location) of density anomaly (σ_t, dark orange); zonal velocity (black); temperature (blue) and salinity (red). For the zonal velocity thick black curves stand for outflow and the thinner for inflow. The sections are plotted for two moments of the wind event, 27th July (a and c) and 6th August (b and d), respectively before and at the peak of the easterlies event (see Fig. 4). (For interpretation of the references to color in this figure legend, the reader is referred to the web version of the article.)

50 m, where a surface cooling is produced in connection with the outcrop of the 17 degree isotherm (see Fig. 4d). However, the inflow shutdown or reversal is noticeable only at the very shallow near-surface levels (see Fig. 4b), and thus any westward transport of cold waters is minimal. The cold band of upwelled water is mostly entrained by the inflow and advected into the Mediterranean; it is not advected offshore to feed the Atlantic side filament.

A daily series of inflow transport (for cross-strait section of Fig. 1a) is represented in Fig. 1b (red line). It shows that the Atlantic inflow responds to the easterlies with a delay of 1–2 days. It is especially clear after the prolonged event ending by 16th July when the inflow reduces to a minimum of 0.47 Sv, a 33% decrease from the mean simulation value (0.7 Sv). However, the inflow reduction after the other events in August is much smaller. We conclude that the upper circulation of the Strait of Gibraltar, which remains eastward, can only transport cold water into the Mediterranean; it has no direct role in the generation of the Atlantic filament.

3.3. *Idealized experiments*

Although the realistic experiments do not present an inflow reversal or shut-off during the Gap wind event, we still need to assess if the filament generation is independent of the Strait flow. More precisely, since we hypothesized that the filament is a product of the upper stratified layer response to a strong and meridionally sheared zonal jet, it should be independent of any coastal upwelling occurring on the southern side of the Strait. To confirm this, we designed additional experiments where the effect of the inflow and the effect of local coastal upwelling inside and near the Strait can be isolated. Two idealised experiments are conducted: The *flat-stratification* case (no horizontal density gradients), and the *no-strait* case. In the *flat-stratification* case, we initialize the ocean with laterally homogeneous temperature and salinity fields typical of summer stratification off the Strait. In the second case, we use the same initialization, but with a flat topography and with closed Strait—a masked Alboran Sea (i.e., no inflow/outflow). Additionally, in this configuration, we prevent a possible influence of coastal divergence associated with meridional winds along the African coast by allowing zonal winds only ($\upsilon = 0$). The remaining forcing conditions are the same as for the real case. Fig. 5 compares the base case with the idealized ones (SST fields) taking the simulation day that corresponds to the peak of easterlies (6th August).

The filament is reproduced in both simulations. In the *flat-stratification* case, there is still a significant contribution of upwelling along the southern side of the Strait (absent in *no-strait* case). There is no advection of colder waters into the Mediterranean basin, since the inflow is no longer active (compare realistic and *flat-stratification* experiments in Fig. 5). In the *no-strait* case, the filament is generated with the same oceanward extention as in the other cases. In this simulation, there is no upwelling neither along the southern coast of the Strait (the Strait is closed), nor along the meridional coast, since the meridional wind component is null everywhere. Finally, in this experiment the filament rotates anticyclonically even more so than in the other cases, since neither the inflow/outflow currents, nor the shelf topography is constraining its development.

The physics behind the filament generation appear very consistent with mechanisms reviewed by Willett et al. (2006; see their sketch on their Fig. 4) to explain the Tehuantepec upwelling system. The mechanisms at work here are illustrated in Fig. 6 presenting the thermal structure along a meridional cross-section, and corresponding zonal surface wind vectors (an isopycnal is also shown). An asymmetric response of the thermocline is produced by Ekman pumping due to wind curl, which creates convergence and divergence zones respectively to the right and left of the wind jet (looking downwind). On the convergence (divergence) side, the thermocline is depressed (lifted), while the sea surface rises (falls). The distortion of the density field then tends to set up geostrophic currents which flow in the direction of the wind near the center of the wind jet, and in the opposite direction on the edges (with cyclonic and anticyclonic tendencies on the left and right sides of the jet, respectively). However, vertical mixing modulate the Ekman pumping effect. In the convergence area, convection mixing associated with advection of lighter over denser water favours the depression of isotherms; on the contrary, the same mixing process weakens the uplifted thermocline in the divergence zone (and enhances surface cooling). As a result, the generation of an anticyclonic eddy is predominant over a weakened (or lacking) cold core cyclonic eddy.

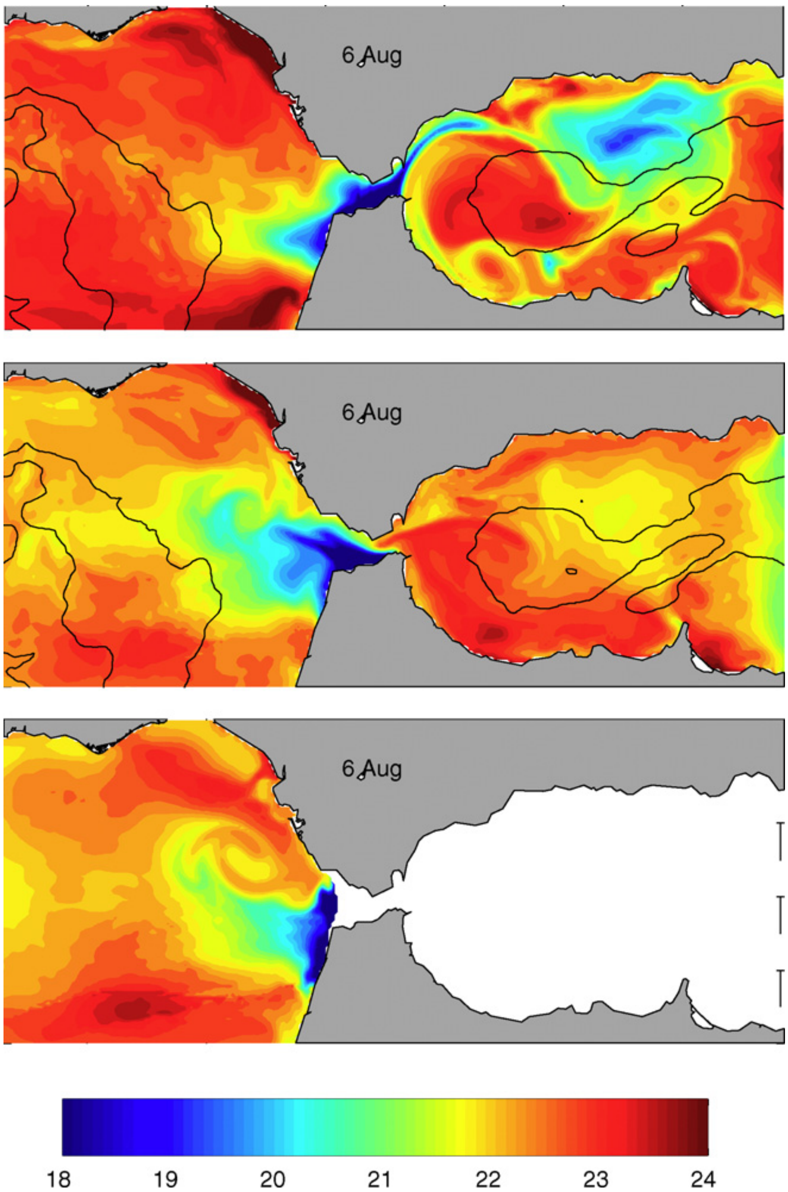

Fig. 5. SST model fields for 6th August from the real case (upper plot); the flat-stratification case (middle plot); and the no-strait case (bottom).

4. Discussion and conclusion

Two independent features occur in response to Levanter winds: upwelling inside the Strait and the development of a cold filament rooted at the southwest corner of the Strait. Model simulations have shown that the upwelling inside the Strait may occur without a significant inversion of the surface dominant inflow and without changing the inflow structure for depths below 50 m. Garcia Lafuente et al. (2002a) come to the same conclusion that full inflow shutdow or inversions are very unusual in the Strait. They mainly occur after large and sudden increases of atmospheric pressure over the western Mediterranean basin, which are more typical in wintertime. The filament formation generates locally and independently of the upwelling inside the Strait. It constitutes a response of the strongly stratified upper layer to Gap wind events associated with Levanter circulation.

The generation and fate of the filament is very similar to the case of Tehuantepec Gulf (Trasvina et al., 1995; Willett et al., 2006), where strong Gap wind events produce an erosion and a deformation of the thermocline that generate anticyclones with space scales in the order of 200 km. The generation of anticyclonic eddies and the lack of cyclonic eddies are well-documented in the case of Gap wind

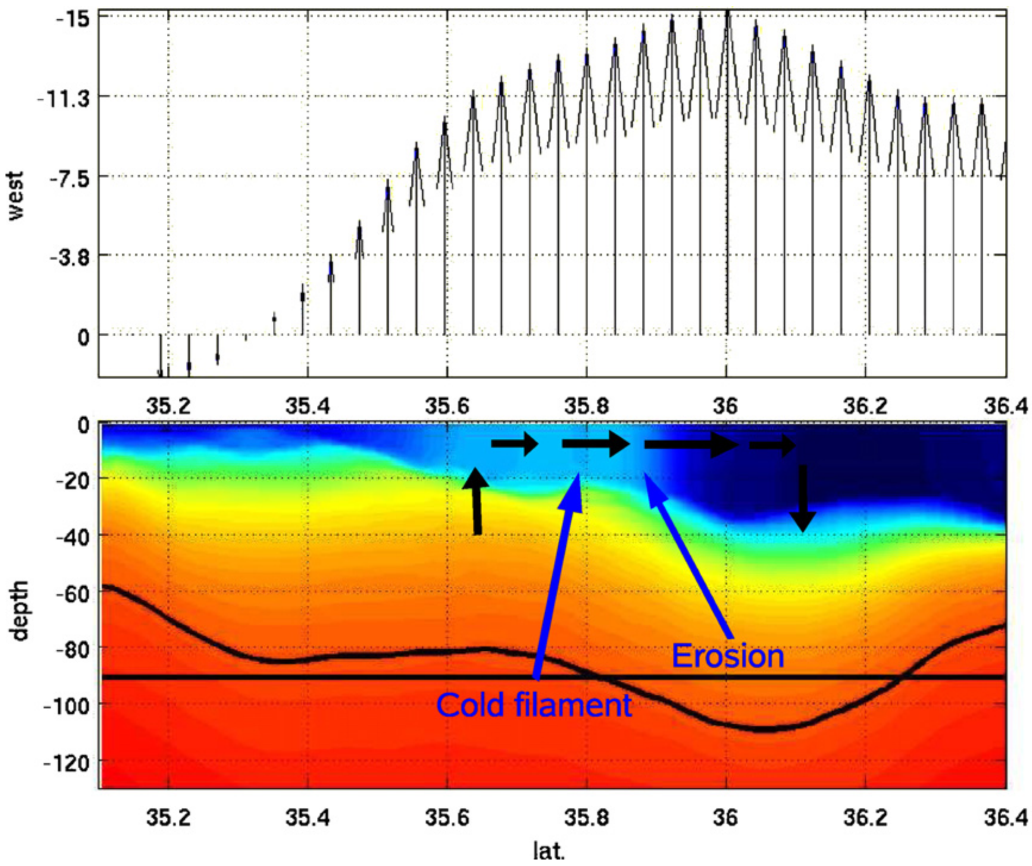

Fig. 6. Zonal wind and upper ocean thermal structure from the no-strait experiment along 6.25 W ("looking" downwind from the Mediterranean). The arrows and labels schematically represent the cross-wind jet circulation that develops in the upper ocean and that is responsible for the filament generation. Thick, black lines represent the 26.8 isopycnal (the flat case stands for the meridional mean) (compare with the cross-wind circulation scheme given in Fig. 4 of Willett et al. (2006)).

events over central America. Our observations and model results suggest that similar phenomena are present in the Gulf of Cadiz, but they are altered by the persisting Atlantic inflow, so that the response to Gap winds is not as dramatic as that reported by (Trasvina et al., 1995).

A description of simulated Levanter events is presented by Capon (2006). The author reports a significant sensitivity of wind intensity to the model spacial resolution. Increasing the resolution from 12 km to 4 km changes the maximum intensity of the jet from around 16 m/s to 18–20 m/s. This may explain the weaker thermal response of our model, since our maximum jet intensity is in the order of 15 m/s. Additionally, in the higher resolution model of Capon (2006), the wind jet is more concentrated near the Strait and a spatial structure is detected which consists of several bands irradiating off the Strait alongwith the main jet. The complex detail in the filaments seen in some satellite imagery (e.g. see the double structure of the filament by day 8th August in Fig. 3, lower plot), may be associated with this spatial organization of the Gap wind jet not accounted for in the present simulation.

In conclusion, we suggest that the filament is a response of the stratified upper layer to the Gap wind jet. Although its SST signature is significant, it has no clear association with an inflow reversal as suggested by Stanichny et al. (2005) for the 2003 period. Short reversals of the inflow have been registered during periods of Levanter (Garcia Lafuente et al., 2002b). Nonetheless and as mentioned above, the bulk of inflow reversal is associated with changes in the spatially averaged surface pressure anomaly over the Western Mediterranean (actual pressure minus the long-term mean) and not with the direct drag of wind acting on the sea surface in the Strait. The anomaly tends to covary negatively with zonal winds in the Strait (positive values would set up negative pressure gradient along the strait and, hence, easterlies) and both effects, pressure anomaly and wind drag, act concomitantly to reduce the inflow. However, these dynamics are still under debate (Garcia Lafuente et al., 2002a).

Acknowledgements

The authors thank the German Aerospace Center (D.L.R.) for providing the satellite imagery. This work was conducted under support of Fundação para a Ciência e a Tecnologia through the research contracts AGuCa (PTDC/MAR/64902/2006) and Clibeco (POCI/CLI/57752/2004). J.G.L. acknowledges partial financial support from Spanish CTM2006-02326 National Project.

References

Armi, L., Farmer, D., 1987. A generalization of the concept of maximal exchange in a strait. Journal of Geophysical Research 92, 14679–14680.

Capon, R., 2006. High resolutions studies of the gibraltar levanter validated using sun-glint anemometry. Meteorological Applications 13, 257–265.

Farmer, D., Armi, L., 1988. The flow of Atlantic water through the Strait of Gibraltar. Progress in Oceanography 21, 1–105.

Folkard, A., Davies, P., Fiúza, A., Ambar, I., 1997. Remotely sensed sea surface thermal patterns in the Gulf of Cadiz and the Strait of Gibraltar: variability, correlations, and relationships with the surface wind field. Journal of Geophysical Research 102, 5669–5683.

Garcia Lafuente, J., Álvarez Fanjul, E., Vargas, J., Ratsimandresy, A., 2002a. Subinertial variability in the flow through the Strait of Gibraltar. Journal of Geophysical Research 107 (C10).

Garcia Lafuente, J., Delgado, J., Criado, F., 2002b. Inflow interruption by meteorological forcing in the Strait of Gibraltar. Geophysical Research Letters 29 (19).

Garcia Lafuente, J., Vargas, J., Baschek, B., Candela, J., Plaza, F., Sarhan, T., 2000. Tides in the eastern section of the Strait of Gibraltar. Journal of Geophysical Research 105 (C6), 14197–14213.

Large, W., McWilliams, J., Doney, S., 1994. Oceanic vertical mixing: a review and model with a nonlocal boundary layer parameterization. Reviews of Geophysics 32 (November (4)), 363–403.

Marchesiello, P., McWilliams, J., Shchepetkin, A., 2003. Equilibrium structure and dynamics of the California Current System. Journal of Physical Oceanography 33 (April (4)), 753–783.

Marchesiello, P., McWilliams, J.C., Shchepetkin, A.F., 2001. Open boundary conditions for long-term integration of regional oceanic models. Ocean Modelling 3 (1–2), 1–20.

Menemenlis, D., Fukumori, I., Lee, T., 2007. Atlantic to Mediterranean sea level difference driven by winds near Gibraltar Strait. Journal of Physical Oceanography 37, 359–376.

Palomares Losada, A., 1999. Analysis of the meteorological synoptic situations that affect the strait of gibraltar and their influence on the surface wind. Boletin del Instituto Espanol de Oceanografia 15, 81–90.

Peliz, A., Dubert, J., Marchesiello, P., Teles-Machado, A., 2007. Circulation in the Gulf of Cadiz: model and mean flow structure. Journal of Geophysical Research 112 (C11015).

Peliz, A., Marchesiello, P., Santos, A., Dubert, J., Teles-Machado, A., Marta-Almeida, M., Le Cann, B., submitted for publication. Circulation in the Gulf of Cadiz. Part 2. Inflow/Outflow coupling and Gulf of Cadiz slope Current.

Penven, P., Debreu, L., Marchesiello, P., McWilliams, J., 2006. Evaluation and application of the ROMS 1-way embedding procedure to the central california upwelling system. Ocean Modelling 12, 157–187.

Sánchez-Román, A., Sannino, G., Garcia Lafuente, J., Carillo, A., Criado Aldeanueva, F., submitted for publication. Transport estimates at the western section of the Strait of Gibraltar: a combined experimental and numerical modelling study. Journal of Geophysical Research.

Send, U., Baschek, B., 2001. Intensive shipboard observatios of the flow through the strait of gibraltar. Journal of Geophysical Research 106 (C12), 31017–31032.

Shchepetkin, A.F., McWilliams, J.C., 2005. The regional oceanic modeling system (roms): a split-explicit, free-surface, topography-following-coordinate oceanic model. Ocean Modelling 9 (4), 347–404.

Skamarock, W. C., Klemp, J. B., Dudhia, J., Gill, D. O., Barker, D. M., Wang, W., Powers, J. G., 2005. Description of the advanced research wrf version 2. NCAR Technical Note NCAR/TN-468+STR, 100 pp.

Stanichny, S., Tigny, V., Stanichnaia, R., Djenidi, S., 2005. Wind driven upwelling along the african coast of the strait of gibraltar. Geophysical Research Letters 32 (L04604).

Teles-Machado, A., Peliz, A., Dubert, J., Sanchez, R., 2007. On the onset of the Gulf of Cadiz coastal countercurrent. Geophysical Research Letters 34 (L12601).

Trasvina, A., Barton, E., Brown, J., Velez, H., Kosro, P., Smith, R.L., 1995. Offshore wind forcing in the Gulf of Tehuantepec, Mexico: the asymetric circulation. Journal of Geophysical Research 100 (C10), 20649–20663.

Vázquez, A., Bruno, M., Izquierdo, A., Macías, D., Ruiz-Cañavate, A., 2008. Meteorologically forced subinertial flows and internal wave generation at the main sill of the Strait of Gibraltar. Deep Sea Research I 55, 1277–1283.

Willett, C., Leben, R.R., Lavin, M., 2006. Eddies and tropical instability waves in the eastern tropical pacific: a review. Progress in Oceanography 69, 218–238.